Chiral perylene materials by ionic self-assembly

Article

Published Version

It is advisable to refer to the publisher's version if you intend to cite from the work. See Guidance on citing.

To link to this article DOI: http://dx.doi.org/10.1021/acs.langmuir.6b02201

Publisher: American Chemical Society

www.reading.ac.uk/centaur

CentAUR

LANGMUIR

Chiral Perylene Materials by Ionic Self-Assembly

Geraldine Echue,*,[†,‡] Ian Hamley,[§] Guy C. Lloyd Jones,[||] and Charl F. J. Faul*,[†]

[†]School of Chemistry, University of Bristol, Bristol BS8 1TS, United Kingdom

[‡]World Premier International (WPI), Research Center for Materials Nanoarchitectonics (MANA), National Institute for Materials Science, 1-1 Namiki, Tsukuba, Ibaraki 305-0044, Japan

[§]Department of Chemistry, University of Reading, Reading RG6 6AD, United Kingdom

[||]School of Chemistry, Joseph Black Building, University of Edinburgh, West Mains Road, Edinburgh EH9 3JJ, United Kingdom

ⓢ *Supporting Information*

ABSTRACT: Two chiral complexes (**1-SDS** and **1-SDBS**) were prepared via the ionic self-assembly of a chiral perylene diimide tecton with oppositely charged surfactants. The effect of surfactant tail architecture on the self-assembly properties and supramolecular structure was investigated in detail using UV−vis, IR, circular dichroism, light microscopy, X-ray diffraction studies, and electron microscopy. The results obtained revealed the molecular chirality of the parent perylene tecton could be translated into supramolecular helical chirality of the resulting complexes via primary ionic interactions through careful choice of solvent and concentration. Differing solvent-dependent aggregation behavior was observed for these complexes as a result of the different possible noncovalent interactions via the surfactant alkyl tails. The results presented in this study demonstrate that ionic self-assembly (ISA) is a facile strategy for the production of chiral supramolecular materials based on perylene diimides. The structure−function relationship is easily explored here due to the wide selection and easy availability of common surfactants.
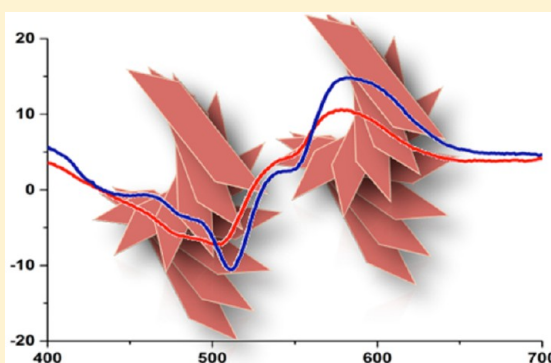
INTRODUCTION

Hierarchical self-assembly of different components into functional superstructures can be found throughout nature, for example, in the formation of cell membranes from proteins, lipids, and steroids, alpha helices and beta sheets as protein secondary structures, as well as light-harvesting photosynthetic systems.[1,2] The preparation of synthetic nanostructured hierarchical materials utilizing the self-assembly route has generated much interest in recent years due to the relative simplicity of this method versus traditional covalent syntheses.[3,4] When focusing on functionality in self-assembled materials, organic π-conjugated materials are candidates of particular interest due to their processability and desirable optoelectronic properties associated with the aromatic systems.[5] Oligomers, polymers, and block copolymers are well-studied materials in this sense, and many self-assembled nanostructures including nanowires,[6] nanoribbons,[7] and nanotubes[8,9] have been prepared and studied in detail.

Perylene diimides (PDIs) and their derivatives are a class of π-conjugated dyes that have been widely investigated for the preparation of functional self-assembled materials due to their application as n-type semiconductors in organic electronic devices and solar cells.[10−12] Selective synthesis of PDI building blocks can be used to tune properties such as solubility, mesophase formation, absorption, and fluorescence quantum yields.[13−15] Strategies commonly employed to influence PDI

properties include variation of side chain length and number, degree of branching, or the inclusion of different functional groups.[16,17]

Substituent modulation is an effective means of controlling the physical and chemical properties of PDIs due to the effect of peripheral substituents on the molecular packing of the central perylene unit.[18−20] Specifically, modification of the imide substituents can be used to incorporate additional noncovalent interactions, thus influencing aggregation, self-assembly, and consequent optoelectronic properties.[21,22]

The incorporation of chiral groups can be used to modify the self-assembly of PDIs due to the additional ordering generated by the spatially specific steric demands of the chiral group. The molecular chirality of the chiral PDI subunits can be translated into supramolecular architectures, resulting in helical supramolecular ordering.[23−25] Biased helical superstructures have been observed for chiral PDIs, the handedness of which can be inverted by the variation of external stimuli such as solvent, temperature, and concentration.[26,27]

Chiral PDIs typically self-assemble to form 1D helical morphologies via rotational stacking of the central perylene cores.[28,29] Other structural motifs observed for self-assembled

Scheme 1. Molecular Structures of the Parent Perylene Tecton 1 (N,N'-bis(2-(trimethylammonium)-3-(phenyl)propyl)-perylene diimide) and the Complexes Synthesized by ISA of Chiral Building Block 1 with C_{12}-Containing Surfactants SDBS and SDS
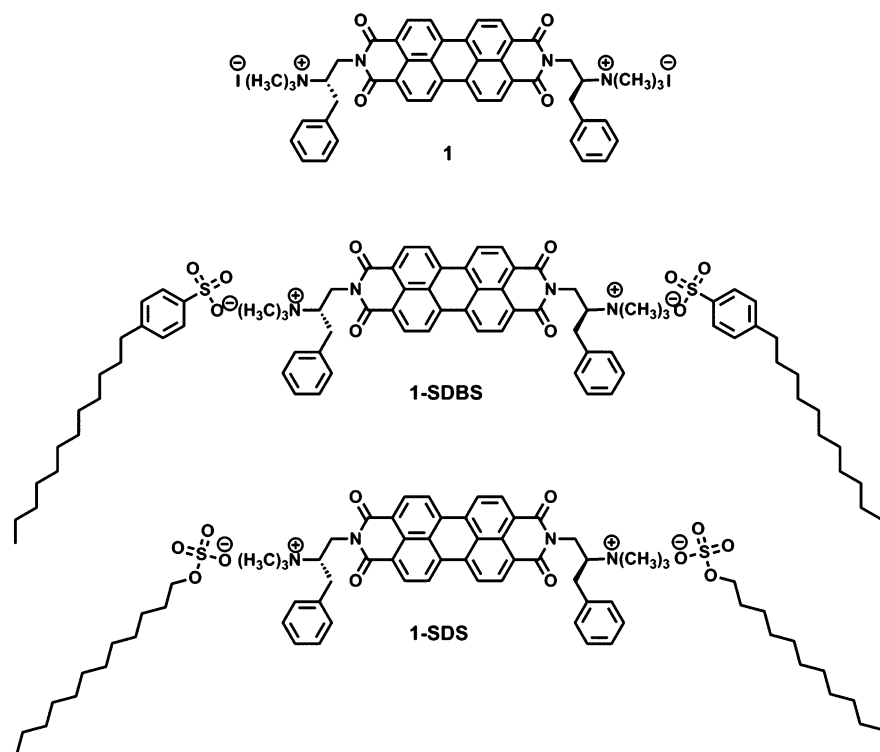
chiral PDIs include chiral pinwheels[30] and spherical nanostructures.[31,32] The most common strategy for the production of chiral PDI materials is by the direct substitution of a chiral group at the imide positions. Chiral moieties including alkyl chains,[33,34] sugars,[35] and amino acids[36−38] have been previously used to prepare supramolecular materials with chiral ordering.

Another strategy for production of chiral PDI materials is by hydrogen bonding of achiral PDIs to chiral molecules to give chiral supramolecular self-assemblies.[39−41] Chiral functional groups such as urea, melamines,[42,43] and oligo(p-phenylenevinylene)s[44] have been utilized for this purpose. Although the use of hydrogen-bonding interactions has been well documented for the formation of chiral self-assembled materials based on PDIs, the use of ionic interactions is much less common. Herein, we describe the use of ionic self-assembly (ISA) for the production of helical chiral materials based on PDIs.

ISA relies on the formation of ordered assemblies via the self-organization of commonly available oppositely charged chemical building blocks (or tectons) such as surfactants, lipids, polyelectrolytes, and polypeptides.[45] The initial driving force for self-assembly is the establishment of primary ionic interactions between the oppositely charged tectons to give charge-neutralized complexes. These complexes can self-assemble into structures of higher complexity via secondary noncovalent interactions such as hydrogen bonding, $\pi-\pi$ interactions, and hydrophobic forces.[46] Functional nano-structured PDI materials have previously been prepared by ISA utilizing combinations of charged PDIs and polyelectrolytes, metal phthalocyanines, or surfactants.[47−49]

Previously, we demonstrated that chiral PDI materials can be prepared by the ISA of achiral perylene derivatives with oppositely charged chiral surfactants.[50,51] The chirality of the

surfactant was transferred to and expressed by the perylene chromophore in the resulting materials; self-organization of the complexes to form helical architectures occurred in both solution and solid state.

In contrast to previous chiral materials synthesized utilizing ISA, here for the first time, we aim to (1) investigate the effect of incorporating the chiral moiety directly into the PDI building block, and (2) explore the ability of the PDI tecton to express chirality in the resulting ISA supramolecular structures coupled through the ionic interactions. Detailed characterization of the self-assembly behavior in both solution and solid state has been carried out to determine the effect of chirality and surfactant structure on the self-assembled structures of the resulting materials.

■ EXPERIMENTAL SECTION

Materials. All chemicals were purchased from Aldrich and used as received unless otherwise specified. Surfactants were used without further purification. 1 (N,N'-bis(2-(trimethylammonium)-3-(phenyl)-propyl)-perylene diimide) was synthesized using a published procedure.[24]

Equipment. ^{1}H and ^{13}C NMR spectra were recorded on a JEOL ECP(Eclipse) 400 spectrometer using the proton signal of TMS or the deuterated solvent as internal standard. All samples were recorded at 20 °C. ESI−mass spectrometry analyses of the samples were performed on a QStar XL Applied Biosystems spectrometer.

Circular dichroism (CD) measurements were obtained with a JASCO-J815 spectropolarimeter. UV−vis data were recorded using a PerkinElmer Lambda 35 UV−vis spectrometer in the range 200−800 nm. Fluorescence measurements were obtained using a Varian Cary spectrophotometer at an excitation wavelength of 470 nm in the range 500−800 nm. Because of the high emission intensity of samples, slit widths of 2.5 and 5 nm were used for EtOH and THF solutions, respectively. All spectra were obtained at rt unless otherwise specified.

Standard 1 or 10 mm path quartz cuvettes were used depending on sample concentration. For spectroscopic measurements in the solid state, films were prepared by casting a THF or EtOH solution (1×10^{-3} M) onto quartz slides, then allowing the solvent to evaporate in air at rt. For electron microscopy measurements, samples were prepared by casting THF or EtOH solution (7.4×10^{-4} M) onto the sample substrate and allowing the solvent to evaporate in air at rt.

Polarized optical microscopy images were obtained using a Nikon BX-50 microscope fitted with an Olympus C-5060 wide zoom digital camera. XRD investigations of the complexes were performed on beamline BM26B (DUBBLE) at the ERSF, Grenoble, France. SAXS data were collected using a Pilatus 1 M detector. For WAXS, a Pilatus 300 K detector was used. The X-ray wavelength was 1.03 Å, and the sample−detector distance was 2 m.

The procedures used for the preparation of the complexes are given in the Supporting Information.

RESULTS AND DISCUSSION

Complexes were prepared by ionic self-assembly of perylene diimide tecton **1** (N,N'-bis(2-(trimethylammonium)-3-(phenyl)propyl)-perylene diimide), with anionic surfactants **SDS** and **SDBS** (to give complexes **1-SDS** and **1-SDBS**, respectively; see Scheme 1). These surfactants are structurally related in that they both possess a single 12-carbon chain. **SDS** and **SDBS** have similar headgroup size and composition, and differ in the linker group between the headgroup and the C_{12} tail, with an aromatic unit for **SDBS** versus an O atom for **SDS**.

Complexation was carried out at elevated temperatures (65 °C) in aqueous solution as temperature-dependent UV−vis studies on the precursor showed that little aggregation of the PDI occurs at this temperature.[24] Thus, preparation was carried out with **1** in the molecularly dissolved state to facilitate complete complexation.

The solubility properties of the resulting surfactant complexes are markedly different from those of the charged parent compound, **1**. Whereas **1-SDS** and **1-SDBS** are highly soluble and exhibit solvatochromism in common organic solvents such as EtOH and THF, precursor **1** is very poorly soluble in EtOH, and insoluble in THF, respectively.

Solution-State Aggregation Behavior. *UV−Vis Investigations.* PDIs are widely known to self-assemble and form aggregates from very low concentrations in poor solvents. The driving force for this low-concentration aggregation phenomenon is the establishment of favorable $\pi-\pi$ interactions between the central aromatic systems. The aggregation geometry of perylenes can be modulated by variation of the imide substituents (in this case, via ionic self-assembly), and can be investigated by UV−vis spectral changes.[52] UV−vis absorption studies were carried out in THF and EtOH to investigate the influence of differences in surfactant structure on the aggregation properties of the complexes in solution.

Both complexes exhibit absorption bands in the 450−550 nm range in EtOH, with distinct vibronic structure associated with the $\pi-\pi^*$ transition observed.[50] Absorption maxima occur at similar values for both complexes at 534, 497, and 465 nm, corresponding to the S_{0-0}, S_{0-1}, and S_{0-2} vibronic transitions, respectively. The appearance of the spectra, that is, absorption maxima of intensity pattern $S_{0-0} > S_{0-1} > S_{0-2}$, is indicative of perylene diimide chromophores in the monomeric state (Figure 1).[34] The ratio of the intensity of the two lowest energy transitions, S_{0-0} and S_{0-1}, can be used to interpret the level of aggregation of perylene chromophores in solution.[53] For aggregated perylene chromophores, typical values for the absorption ratio A_{0-0}/A_{0-1} are <0.7. Monomerically dissolved
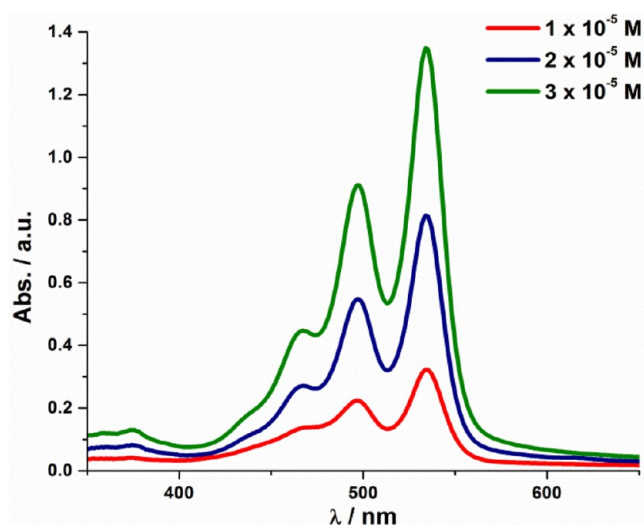
Figure 1. Concentration-dependent UV−vis absorption spectra for **1-SDS** in EtOH. Similar curves were obtained for **1-SDBS** (see Figure S1).

PDIs exhibit normal Franck−Condon progression with a ratio A_{0-0}/A_{0-1} of ca. 1.6.[54]

The absorption ratios obtained for **1-SDS** and **1-SDBS** indicate that the complexes are nonaggregated at low concentration in EtOH. It is likely that EtOH is a good solvent for these complexes due to the hydrogen-bonding capability of the carbonyl groups of the imide units and the oxygen-rich headgroups of the surfactants (i.e., hydrogen-bonding acceptors).[51] Although the decrease in the absorption ratios indicates that the aggregation of the chromophores increases with concentration (Table S1), the absorption maxima remained constant over the concentration range assayed (1×10^{-5} to 1×10^{-3} M). At lower concentration (1×10^{-6} M), **1-SDS** exhibits the highest tendency for aggregation, whereas the level of aggregation for both complexes is comparable at higher concentration (1×10^{-4} M). It could be expected that the extra oxygen atom in **1-SDS** would afford greater solubility in EtOH due to greater capacity for hydrogen bonding; however, it is possible that the absence of a bulky aromatic group in the surfactant tails of **1-SDS** gives rise to more efficient packing of the PDI complexes, thus leading to increased aggregation. Conversely, it is likely that favorable $\pi-\pi$ interactions of the aromatic ring of **SDBS** play a greater role with increasing concentration, thus overcoming the steric crowding effects and leading to levels of aggregation similar to those found for **1-SDS**.

In contrast to the bright orange colors of the solutions dissolved in EtOH, deep purple solutions were obtained when THF was used as solvent. For both complexes, the S_{0-1} transition now occurs with the highest intensity (Figure 2); this pattern of absorption is consistent with perylene chromophores in the aggregated state. When highly aggregated, there are very strong ground-state interactions between the molecules, and the Franck−Condon factors now favor the S_{0-1} excited vibronic state.[55]

In THF, reduced UV−vis absorption intensity was observed relative to the spectra obtained in EtOH. Broadening of the peaks in the spectra occurs, indicative of increased excitonic coupling of the chromophores in the aggregates.[56] **1-SDS** and **1-SDBS** exhibit a similar general absorption pattern with an absorption maximum at 507 nm for the S_{0-1} transition. The
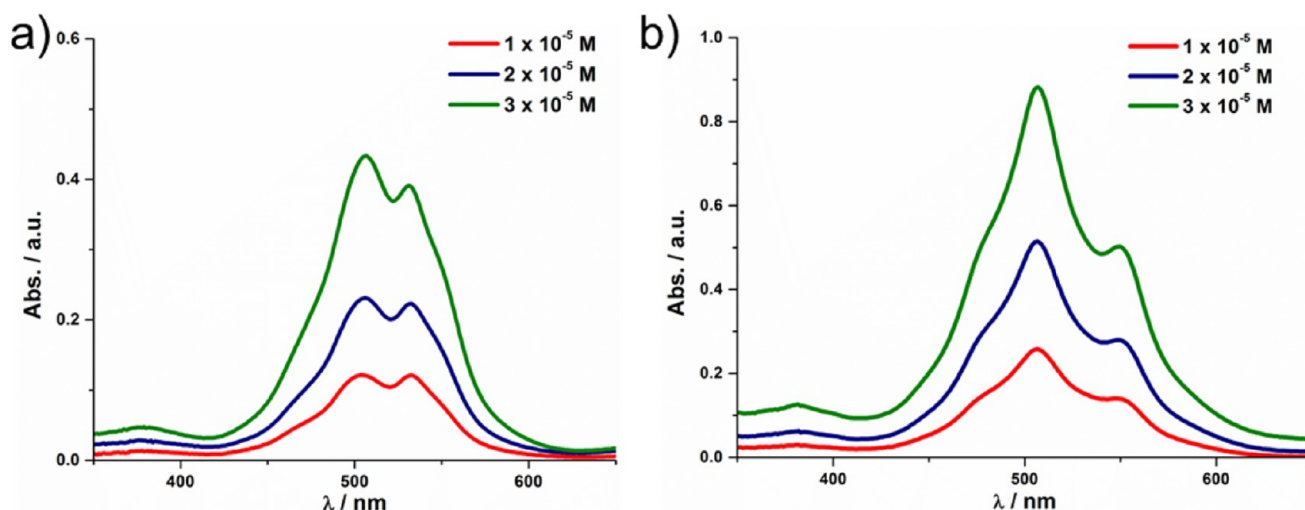
Figure 2. Concentration-dependent UV−vis absorption spectra for complexes in THF: (a) **1-SDS** and (b) **1-SDBS**.
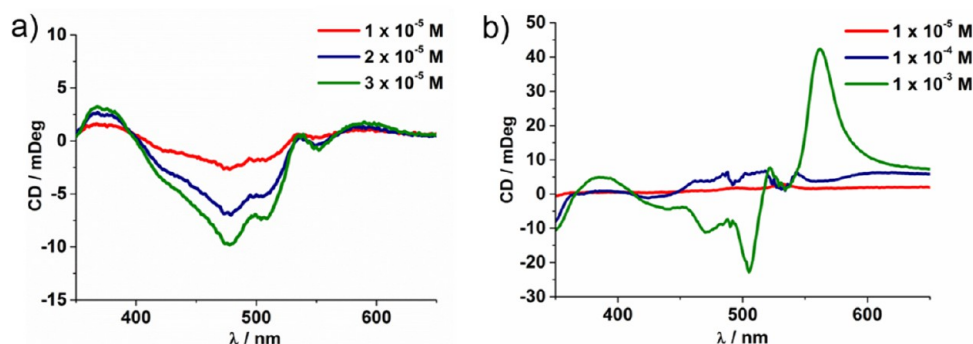
Figure 3. Concentration-dependent CD spectra in EtOH: (a) for **1-SDS** and (b) **1-SDBS** (1×10^{-5}, 1×10^{-4} M were measured using a 10 mm path; 1×10^{-3} M was measured using a 1 mm path).

absorption bands are also bathochromically shifted relative to the equivalent transitions of the complexes dissolved in EtOH.

With increasing concentration, the intensity of the lower energy S_{0-0} transition diminishes with respect to the S_{0-1} transition. The blue shift of the λ_{max} absorption relative to the monomeric state is characteristic of the formation of H-aggregates in which the perylene units are stacked with cofacial geometry.[52] In addition to the blue shift of the absorption maximum, a new absorption feature starts to form as a shoulder initially at ca. 550 nm for **1-SDS**, which is associated with the increased aggregation of the perylene chromophores. At the same time, the absorption peak at 530 nm begins to decrease in intensity (Figure 2b, Figure S1b). The absorption ratios measured in THF indicate that **1-SDBS** is more highly aggregated than **1-SDS** at low concentration. The monomer peak at 530 nm is absent for **1-SDBS**, and the absorption maximum for the S_{0-0} transition occurs at 549 nm throughout the entire concentration range investigated (1×10^{-5} M to 1×10^{-3} M). In contrast, this higher wavelength peak only becomes more pronounced for **1-SDS** at concentrations above 1×10^{-4} M.

According to the molecular exciton theory, the spectral features for these complexes are dependent upon the angle of the center-to-center vector of the transition dipole moments.[57] The appearance of both red- and blue-shifted bands in the spectra has previously been observed in other H-aggregated PDI systems, and is likely due to rotational offset of the

transition dipoles of the stacked perylene cores as opposed to a strictly parallel confirmation.[56]

Although THF is a good hydrogen-bond acceptor, the lack of hydrogen-bond donors in this solvent reduces its ability to solvate the PDI complexes. Hence, the central aromatic cores have a higher preference for $\pi-\pi$ stacking in THF as compared to EtOH at the same concentrations (Table S2). The A_{0-0}/A_{0-1} ratios indicate that at both high and low concentrations, **1-SDBS** exhibits the highest tendency for aggregation.

Circular Dichroism Investigations. Circular dichroism (CD) studies were carried out to investigate whether the chirality of the designed and synthesized PDI tecton can be expressed in the self-assembled structure of the supramolecular complexes. CD measurements of the parent perylene tecton **1** in H_2O at a range of concentrations gave a bisignate absorption signal, which varied from positive to negative with increasing wavelength.[4] This feature corresponds to an arrangement of the transition dipoles of the perylene chromophores in a right-handed helical fashion.[26,50]

The CD spectra of the complexes were measured in both EtOH and THF. At low concentration, **1-SDBS** exhibited weak Cotton effects in EtOH (Figure 3b); the absorption observed was positive only and thus clearly indicates the absence of supramolecular chiral helical aggregates of the chromophore for this complex in EtOH. The CD spectra obtained for **1-SDBS** in EtOH were in good agreement with UV−vis measurements, which were characteristic of nonaggregated perylene diimide chromophores in solution. Instead, it is likely that any
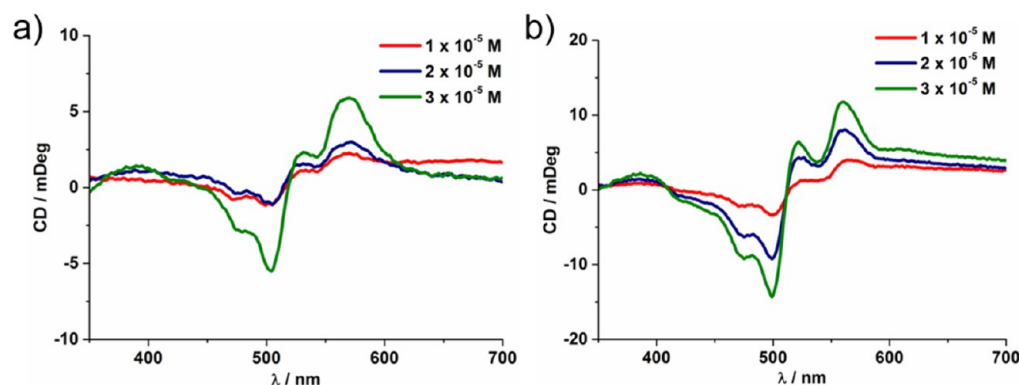
Figure 4. Concentration-dependent CD spectra in THF for (a) **1-SDS** and (b) **1-SDBS**.
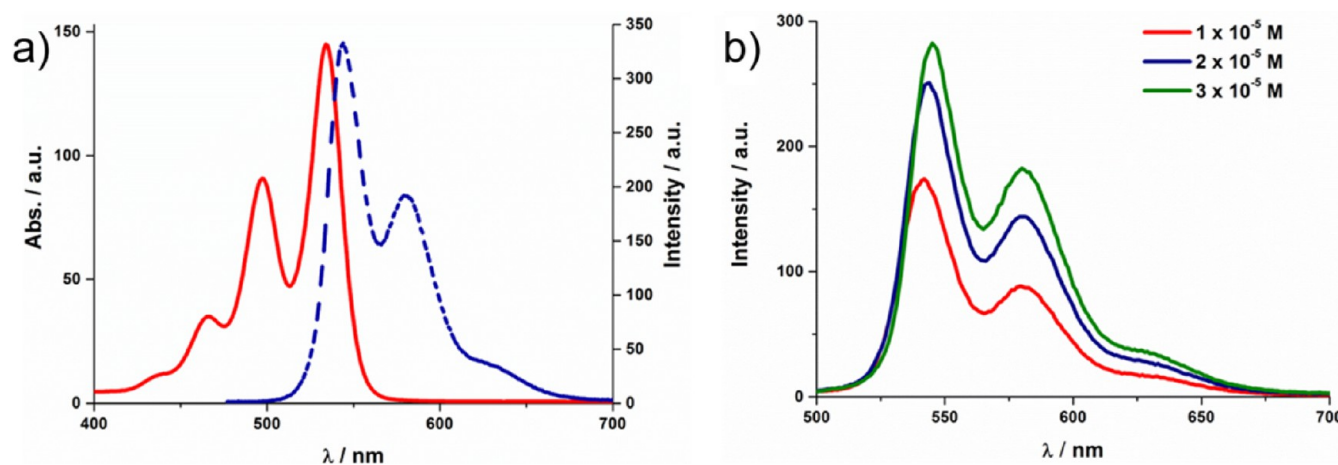

Figure 5. Mirror UV–vis (right axis) and fluorescence spectrum (left axis) in EtOH of (a) **1-SDBS**, $c = 3 \times 10^{-5}$ M. (b) Concentration-dependent fluorescence spectra in EtOH for **1-SDS**, excitation wavelength = 470 nm, slit width 2.5 nm.

aggregates formed by **1-SDBS** are transient and disordered, hence giving rise to the weak Cotton effects in the CD spectra.

For **1-SDS**, different absorption behavior is observed in the CD spectrum in EtOH as compared to **1-SDBS** (Figure 3a and b, respectively). The spectra reveal a weakly bisignate Cotton effect is induced in the **1-SDS** perylene chromophore in EtOH at low concentration (1×10^{-5} M). UV–vis measurements indicated that **1-SDS** is more aggregated relative to **1-SDBS** at low concentration in EtOH (see Table S1); the appearance of a bisignate Cotton effect for **1-SDS** at low concentration follows this trend and reflects the greater ability of this complex to self-assemble into helical architectures at low concentration in EtOH versus **1-SDBS**.

The absorption ratios from the UV–vis spectra in EtOH indicated that the level of aggregation increases with increased concentration for both complexes. For **1-SDBS**, the transition from disordered chiral aggregates to right-handed helical aggregates occurs upon increasing concentration, as evidenced by the appearance of a characteristic bisignate signal by CD at 1×10^{-3} M (Figure 3b). For **1-SDS**, the intensity of the bisignate Cotton effect increases with concentration, clearly indicating right-handed helical architectures for this complex throughout the concentration range assayed.

In THF, the aggregation of the complexes is more enhanced and the CD signals observed are of greater intensity in comparison to those obtained in EtOH at the same concentrations. Clearly resolved bisignate Cotton effects occur throughout the entire concentration range assayed in

THF (1×10^{-5} to 1×10^{-3} M) for both **1-SDS** and **1-SDBS** (Figure 4a and b, respectively). The CD signal measured for **1-SDBS** is of greater intensity as compared to **1-SDS** in THF, and confirms the increased tendency for aggregation in this system (as was also found by UV–vis spectroscopy). The positive sign of the couplet in the CD spectra obtained in THF for both complexes indicates that the perylene chromophore is oriented in a right-handed helical fashion in the self-assembled structures formed.

Fluorescence Investigations. As changes in the aggregation of the chromophores can influence their emission spectra, concentration-dependent fluorescent measurements were carried out in both THF and EtOH to further characterize the aggregation behavior in these solvents.

Photoluminescence spectra obtained in EtOH exhibited well-defined vibronic structure for both complexes. At each concentration assayed, the fluorescence spectrum is approximately a mirror image of the absorption spectrum (Figure 5a). The pattern of emission in EtOH for each complex is almost identical with λ_{max} values occurring at 545 and 580 nm and a relatively small Stokes shift of 10 nm. Upon increasing concentration, very little change occurs in the spectral features for both complexes. The spectra obtained for **1-SDS** and **1-SDBS** are characteristic of PDI systems in which little aggregation is occurring and the PDI is predominantly in the monomeric form (see Figure 5b as an example).

Photoluminescence spectra obtained in THF indicated lower emission intensity for the complexes relative to measurements
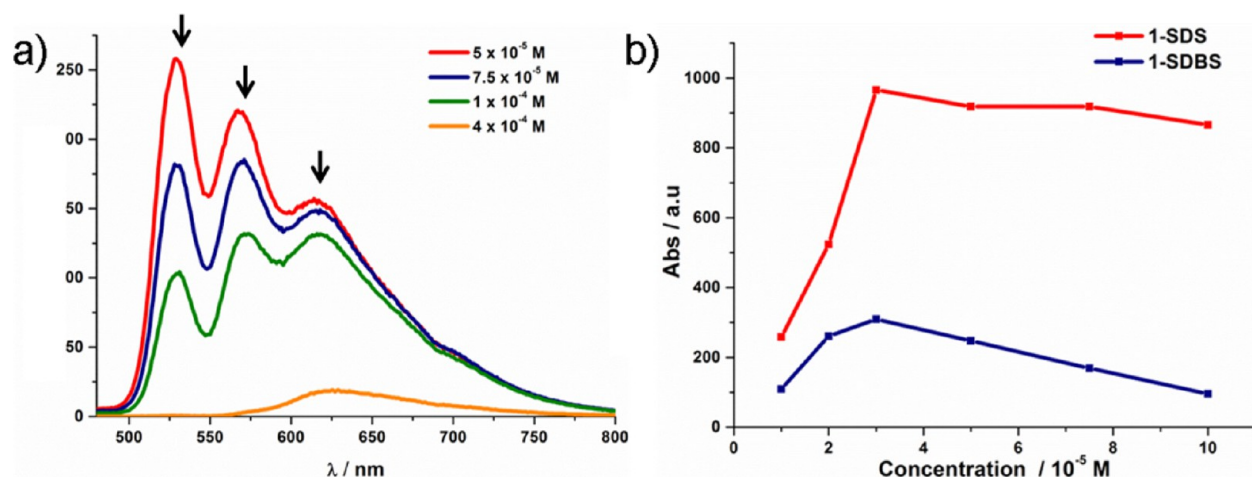
Figure 6. (a) Concentration-dependent fluorescence spectra of **1-SDBS** in THF, $c = 5 \times 10^{-5}$ to 4×10^{-4} M, arrows indicate changes with increasing concentration, see Figure S3 for **1-SDS** data; and (b) changes in the photoluminescence of the lowest wavelength emission band with concentration for the complexes in THF, excitation wavelength 470 nm, slit width 5 nm.
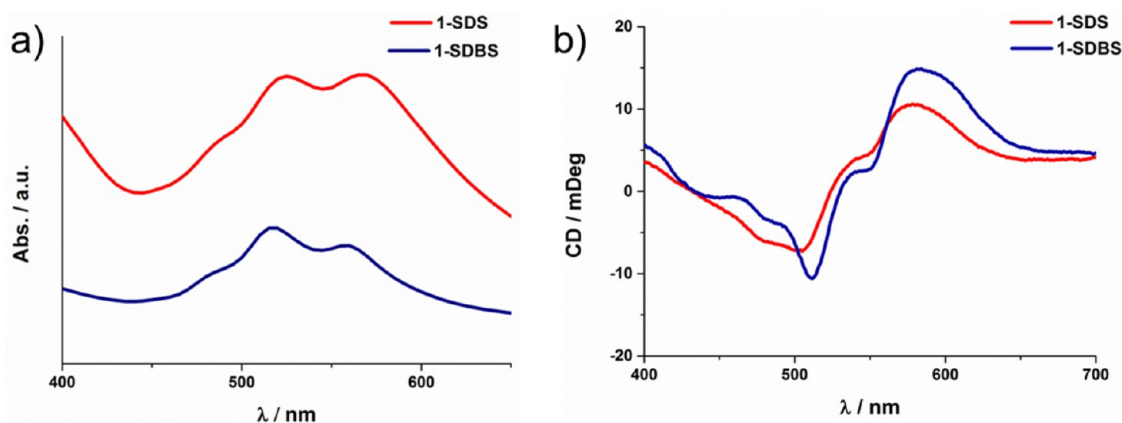

Figure 7. Spectroscopic properties of the films cast of the complexes: (a) UV−vis absorption of films cast from EtOH; and (b) CD spectra of films cast from 1×10^{-3} M THF solutions.

obtained in EtOH. **1-SDS** exhibited greater emission intensity at low concentration versus **1-SDBS**, likely due to the reduced aggregation of the latter complex as was already indicated by the UV−vis measurements in THF. Emission bands were observed in the 500−650 nm range for both complexes, with emission maxima at 525 and 559 nm. Similar spectral patterns were obtained for both complexes at low concentration (1×10^{-5} to 3×10^{-5} M), in which the emission intensity increases with concentration until a threshold value is reached (3×10^{-5} M in both cases, see below); further increases above this threshold concentration led to fluorescence quenching. Although this threshold concentration occurs at 3×10^{-5} M for both complexes, different patterns of fluorescence quenching are observed above the threshold for each complex. For **1-SDS**, the fluorescence intensity of the lowest wavelength emission band remains virtually constant between 3×10^{-5} and 1×10^{-4} M, whereas the fluorescence intensity of the same peak for **1-SDBS** diminishes at a faster rate within this concentration interval (Figure 6b). For **1-SDBS**, the intensity of all three emission bands begins to diminish above 3×10^{-5} M, and at concentrations of 4×10^{-4} M, a broad shoulder begins to emerge at 608 nm (Figure 6a). The differences in fluorescence intensity with concentration for **1-SDS** and **1-SDBS** are indicative of different aggregation behavior for the

complexes. At the highest concentration assayed (4×10^{-4} M), the fluorescence intensity is almost completely quenched for both complexes; however, whereas for **1-SDBS** a single broad structureless emission band occurs at this concentration, for **1-SDS** vibronic structure can still be observed in the spectrum (see Figure S3). For PDIs, loss of vibronic structure is commonly observed due to increased excitonic coupling as a result of chromophores, which are stacked in close proximity.[58,59] The lack of vibronic structure for the emission spectra of **1-SDBS** at high concentration is indicative of the increased aggregation of this complex. For both complexes, the loss in fluorescence intensity is likely due to a self-quenching mechanism as a result of reabsorption of the emission by aggregated molecules in the ground state.

Aggregation Behavior in Films. *UV−Vis Investigations.* Films of the complexes were prepared by drop casting 1×10^{-3} M solutions of the complex onto quartz plates. UV−vis and CD spectra were recorded to investigate whether the self-assembly and aggregation of the molecules in solution could be preserved in the solid state. For both complexes (Figure 7), films cast from either EtOH or THF gave spectra similar to those of the complexes in THF solution (see Figure 7); the UV−vis spectra of these films exhibited broad, poorly defined absorption bands, and the vibronic structure was much less resolved. The
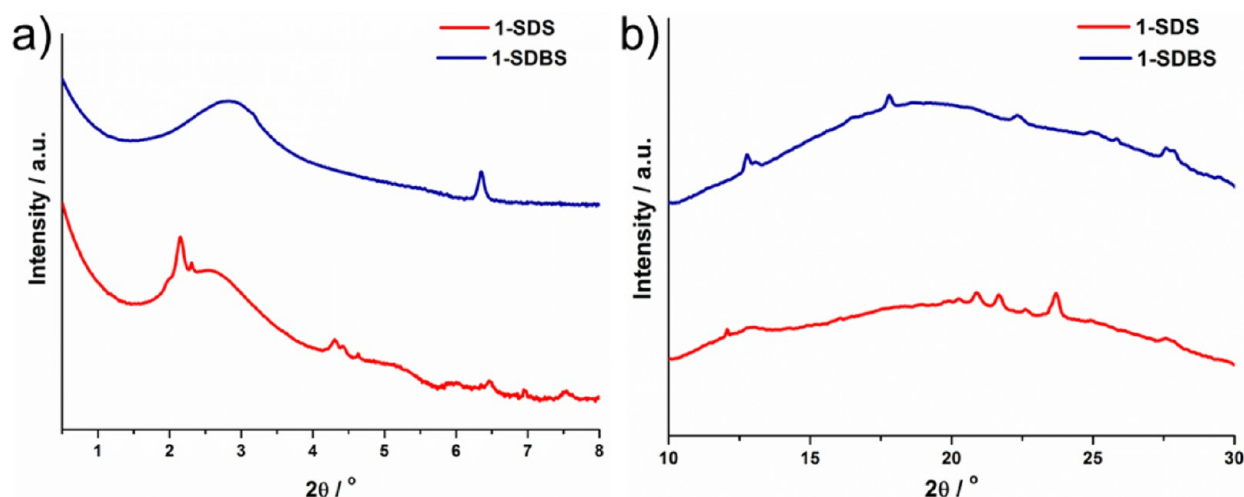
Figure 8. X-ray diffraction studies of the films cast from EtOH: (a) SAXS, and (b) WAXS.

hypsochromic shift of the absorption maximum to the S_{0-1} transition is characteristic of perylene chromophores stacked cofacially in the aggregated state. These spectra indicate that the packing features of the self-assembled aggregates in solution are conserved in the solid state for both complexes.

CD Investigations. CD measurements of the solid-state films cast from THF for both complexes (shown in Figure 7b) showed features similar to those obtained in THF solution (Figure 3). Each complex exhibited a bisignate Cotton effect characteristic of right-handed helical orientation of the transition dipoles in the films upon aggregation.

Similarly to the behavior seen at high concentration in EtOH, **1-SDBS** films cast from EtOH exhibited strong bisignate Cotton effects; that is, the chromophores are in a strongly aggregated state. The absorption maxima and minima were identical to those observed for the THF films. Films of **1-SDS** cast from EtOH also showed characteristics similar to those observed in EtOH solution, with a weakly bisignate Cotton effect evident (see Figure S4). This corresponds with the pattern of absorption observed in the UV–vis data for this complex, indicating that the helical ordering of the aggregates in solution was clearly preserved in the solid state.

Bulk Aggregation Behavior. *General Characterization.* Temperature-dependent polarized optical microscopy (POM) was used to further characterize the films of the complexes cast from THF and EtOH (Figure S5). POM revealed highly birefringent materials at room temperature, indicative of anisotropic organization of the complex materials for films cast from both solvents. A liquid-crystalline phase structure could not be assigned to the films as the domains were very small. No transitions to the isotropic state prior to the onset of degradation were observed for either of the complexes. Thermal annealing could therefore not be used to investigate the mesophase character of the materials.

X-ray diffraction (XRD) was carried out on films cast from EtOH solutions to further investigate the structural ordering within the materials (Figure 8). Wide-angle X-ray scattering (WAXS) analysis of **1-SDS** films cast from EtOH indicated that the π–π stacking was strongly reduced when compared to the π–π stacking typically observed in PDI systems.[11] A low intensity diffraction peak is observed at $2\theta = 27.29°$, giving a π–π stacking distance of 3.27 Å. Peaks corresponding to

crystalline packing of the alkyl tails occur at $2\theta = 20.8–23.7°$ (Figure 8b).

Small-angle X-ray scattering (SAXS) analysis of **1-SDS** gave a broad reflection centered on $2\theta = 2.6°$; superimposed on this reflection is a higher intensity sharp reflection at $2\theta = 2.14°$. A set of reflections at integer multiples of this angle points to the presence of lamellar ordering, although there are also a series of broader reflections pointing to a coexistence of structures of lower order. These results indicate that mixed phases exist for **1-SDS** films.

Similar, for **1-SDBS**, a very low intensity reflection occurs at $2\theta = 27.2°$, which corresponded to a π–π stacking distance of 3.28 Å for the complex. The absence of strong reflections (and presence of a broad scattering halo) in the region corresponding to the alkyl tails is likely to be indicative of a disordered arrangement of the alkyl chains in this complex. SAXS analysis of the material gave a very broad peak at $2\theta = 2.82°$ corresponding to a structural feature of 31.1 Å, as well as an additional (unidentified) scattering feature at $2\theta = 6.5°$. Overall the SAXS results were representative of little long-range ordering within the films cast from EtOH for this complex.

Electron Microscopy. Electron microscopy investigations were carried out to observe the self-assembled structures of the complexes in thin films. It was aimed to investigate the effect of the different structural compositions of the surfactant alkyl tails on the self-assembly of the ISA complexes.

TEM micrographs of thin films for both complexes cast from either EtOH or THF (Figures S6 and S7) showed similar morphologies: sheet-like architectures consisting of smaller aggregates of nonuniform width and length. Because of the sheet-like morphology, helical ordering could not be identified in the self-assembled structures. It was therefore decided to expand our investigations, and explore whether solvent could be used as a driving force for the formation of well-defined self-assemblies for the complexes. We utilized a solution-injection method in which the complexes in "good" solvent were added to "poor" solvent with vigorous mixing. EtOH was chosen for the good solvent as spectroscopic studies demonstrated that the PDI complexes were molecularly dissolved in EtOH solution. Water was chosen as the poor solvent as the complexes exhibit little solubility in aqueous solution.

Four different conditions were employed (80/20, 50/50, 20/80, and 4/96 EtOH and water). A well-defined spherical
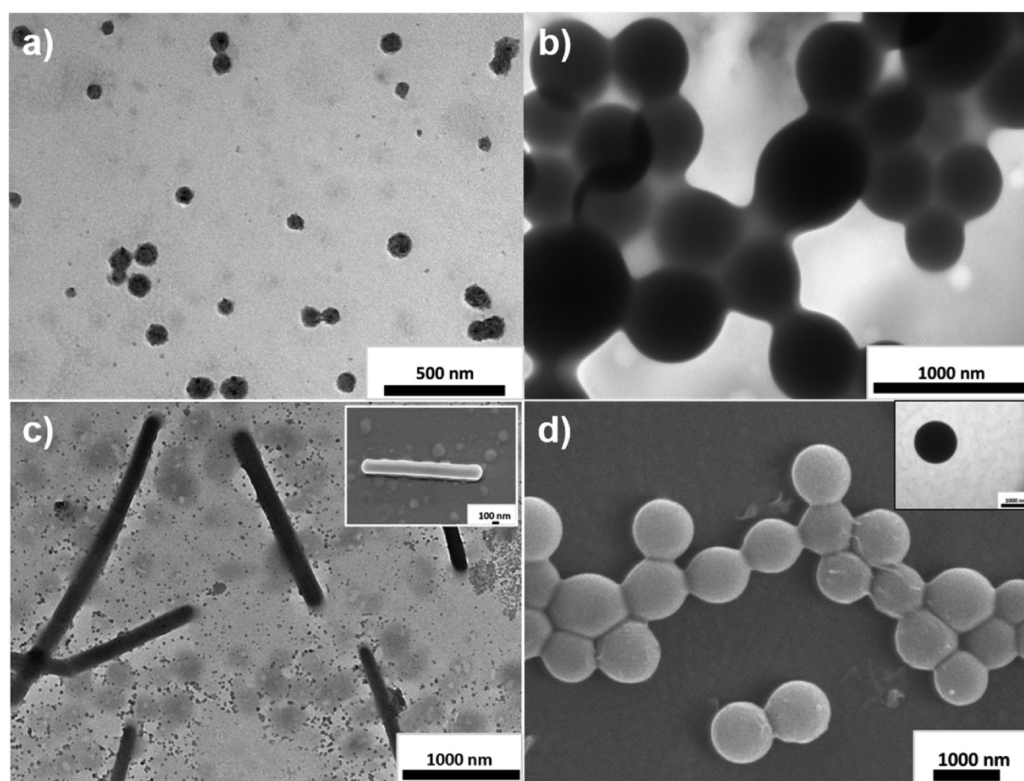
Figure 9. TEM and SEM images of self-assembled structures of the complexes produced using different solvent compositions of EtOH:Water for (a) **1-SDS** 4/96, (b) **1-SDS** 50/50, (c) **1-SDBS** 4/96, and (d) **1-SDBS** 50/50.

morphology was observed for both complexes across the conditions with the three highest proportions of water (Figure 9, Figures S8 and S9). With decreasing proportion of EtOH (and thus decreasing concentration of each complex), the spherical aggregates decrease in size, and increasingly depart from the observed spherical structures.

Films of each complex were prepared from a 50:50 EtOH:Water system, and were analyzed by UV and CD, to probe the structure of the observed aggregates. For both **1-SDS** and **1-SDBS**, UV spectroscopic analysis indicated that the perylene cores adopt an H-aggregate mode of packing in the spherical self-assemblies (Figure S10). CD analysis of the films was indicative of a right-handed helical arrangement of the perylene units in the spherical aggregates (Figure S11). Helical ordering has previously been reported for chiral PDI systems forming self-assembled spherical aggregates.[60]

Interestingly, TEM investigations revealed the existence of different architectures for **1-SDS** versus **1-SDBS** at high water content and low concentration (4/96 EtOH:Water). For **1-SDS**, spherical structures were obtained (Figure 9a), whereas **1-SDBS** exhibited rod-like structures (Figure 9c). The lengths of the rods varied widely, but the widths were uniform at ∼100 nm for **1-SBDS**.

For PDIs, ordered 1D stacking takes place due to a balance between the lateral interactions between the side chains (in this case, the extended side chains from the surfactant tails) and the tendency for $\pi-\pi$ stacking between the central perylene units. At higher volume fractions of poor solvent, the hydrophobic driving force for aggregation is increased, and $\pi-\pi$ interactions between the central perylene units direct the formation of self-assembled complex aggregates. For **1-SDBS**, $\pi-\pi$ interactions in addition to van der Waals forces can occur between the surfactant alkyl tails as a result of the benzyl moieties. Both of

these interactions stabilize the self-assembly into 1D columnar arrays, and could provide a possible explanation for the formation of rods over spheres. The hydrophobic effect also drives the formation of aggregates for **1-SDS**; however, other than van der Waals interactions, there are few other secondary interactions to direct the self-assembly in a columnar fashion. Control experiments carried out using the parent compound **1** did not give any well-defined spherical nanostructures, providing further evidence that the self-assembly in the solvent systems used here is highly dependent upon the presence of the oppositely charged surfactants (Figure S12).

With increasing proportion of EtOH, the hydrophobic driving force for aggregation is reduced, leading to distorted $\pi-\pi$ stacking geometries for the complexes. Instead of 1D self-assembly, spherical morphologies are obtained for both complexes, the size of which increases with concentration.

■ CONCLUSION

We have presented the preparation of chiral supramolecular materials using the ionic self-assembly of oppositely charged surfactants with an intrinsically chiral perylene diimide tecton, **1**. The differences in the solubility and aggregation properties of the parent tecton versus those of the complexed materials illustrate how the ISA strategy can be used to tune the properties of chiral perylene diimides via rational selection of precursors. Characterization of the materials indicates that the properties of the parent tectons can be conserved utilizing ionic interactions; in particular, the molecular chirality of the perylene tecton can be translated into the molecular chirality of the resulting materials. The differences in surfactant tail architecture enabled specific noncovalent interactions that influenced the aggregation behavior and self-assembly of the

complexes in solution and solid state, leading to the formation of a range of morphologies (depending on preparation conditions). X-ray diffraction demonstrated the presence of mixed phases for the complexes in the solid state.

These results illustrate the potential of the ISA strategy for the generation of a library of materials without covalent synthesis based on the chiral tecton **1**, in which the dominant chiral features are preserved when using commonly available oppositely charged surfactants. In this way, ISA represents a particularly attractive route for the preparation of chiral functional materials based on PDIs, for the investigation of the relationship between structure, function, and application.

■ ASSOCIATED CONTENT

ⓢ Supporting Information

The Supporting Information is available free of charge on the ACS Publications website at DOI: 10.1021/acs.langmuir.6b02201.

> Full synthesis details, further spectroscopic measurements, and morphological characterization of the self-assembled structures (PDF)

■ AUTHOR INFORMATION

Corresponding Authors
*E-mail: echue.geraldine@nims.go.jp.
*E-mail: charl.faul@bristol.ac.uk.
Notes
The authors declare no competing financial interest.

■ ACKNOWLEDGMENTS

■ REFERENCES

(1) Zhang, S. Fabrication of novel biomaterials through molecular self-assembly. *Nat. Biotechnol.* **2003**, *21* (10), 1171−1178.

(2) Cornelissen, J.; Rowan, A. E.; Nolte, R. J. M.; Sommerdijk, N. Chiral architectures from macromolecular building blocks. *Chem. Rev.* **2001**, *101* (12), 4039−4070.

(3) Ariga, K.; Li, J. B.; Fei, J. B.; Ji, Q. M.; Hill, J. P. Nanoarchitectonics for Dynamic Functional Materials from Atomic-/Molecular-Level Manipulation to Macroscopic Action. *Adv. Mater.* **2016**, *28* (6), 1251−1286.

(4) Krieg, E.; Rybtchinski, B. Noncovalent Water-Based Materials: Robust yet Adaptive. *Chem. - Eur. J.* **2011**, *17* (33), 9016−9026.

(5) Hoeben, F. J. M.; Jonkheijm, P.; Meijer, E. W.; Schenning, A. About supramolecular assemblies of pi-conjugated systems. *Chem. Rev.* **2005**, *105* (4), 1491−1546.

(6) Bell, O. A.; Wu, G.; Haataja, J. S.; Brömmel, F.; Fey, N.; Seddon, A. M.; Harniman, R. L.; Richardson, R. M.; Ikkala, O.; Zhang, X.; Faul, C. F. J. Self-Assembly of a Functional Oligo(Aniline)-Based Amphiphile into Helical Conductive Nanowires. *J. Am. Chem. Soc.* **2015**, *137* (45), 14288−14294.

(7) Kim, F. S.; Ren, G. Q.; Jenekhe, S. A. One-Dimensional Nanostructures of pi-Conjugated Molecular Systems: Assembly, Properties, and Applications from Photovoltaics, Sensors, and Nanophotonics to Nanoelectronics. *Chem. Mater.* **2011**, *23* (3), 682−732.

(8) Ajayaghosh, A.; Varghese, R.; Mahesh, S.; Praveen, V. K. From vesicles to helical nanotubes: A sergeant-and-soldiers effect in the self-assembly of oligo(p-phenyleneethynylene)s. *Angew. Chem., Int. Ed.* **2006**, *45* (46), 7729−7732.

(9) Palmer, L. C.; Stupp, S. I. Molecular Self-Assembly into One-Dimensional Nanostructures. *Acc. Chem. Res.* **2008**, *41* (12), 1674−1684.

(10) Huang, C.; Barlow, S.; Marder, S. R. Perylene-3,4,9,10-tetracarboxylic Acid Diimides: Synthesis, Physical Properties, and Use in Organic Electronics. *J. Org. Chem.* **2011**, *76* (8), 2386−2407.

(11) Würthner, F.; Saha-Möller, C. R.; Fimmel, B.; Ogi, S.; Leowanawat, P.; Schmidt, D. Perylene Bisimide Dye Assemblies as Archetype Functional Supramolecular Materials. *Chem. Rev.* **2016**, *116* (3), 962−1052.

(12) Zhan, X. W.; Facchetti, A.; Barlow, S.; Marks, T. J.; Ratner, M. A.; Wasielewski, M. R.; Marder, S. R. Rylene and Related Diimides for Organic Electronics. *Adv. Mater.* **2011**, *23* (2), 268−284.

(13) Yagai, S.; Usui, M.; Seki, T.; Murayama, H.; Kikkawa, Y.; Uemura, S.; Karatsu, T.; Kitamura, A.; Asano, A.; Seki, S. Supramolecularly engineered perylene bisimide assemblies exhibiting thermal transition from columnar to multilamellar structures. *J. Am. Chem. Soc.* **2012**, *134* (18), 7983−94.

(14) Tam-Chang, S.-W.; Helbley, J.; Iverson, I. K. A study of the structural effects on the liquid-crystalline properties of ionic perylenebis(dicarboximide)s using UV-vis spectroscopy, polarized light microscopy, and NMR spectroscopy. *Langmuir* **2008**, *24* (5), 2133−2139.

(15) Sun, M.; Mullen, K.; Yin, M. Water-soluble perylenediimides: design concepts and biological applications. *Chem. Soc. Rev.* **2016**, *45* (6), 1513−1528.

(16) Chen, Z. J.; Lohr, A.; Saha-M?ller, C. R.; Wurthner, F. Self-assembled pi-stacks of functional dyes in solution: structural and thermodynamic features. *Chem. Soc. Rev.* **2009**, *38* (2), 564−584.

(17) Balakrishnan, K.; Datar, A.; Naddo, T.; Huang, J. L.; Oitker, R.; Yen, M.; Zhao, J. C.; Zang, L. Effect of side-chain substituents on self-assembly of perylene diimide molecules: Morphology control. *J. Am. Chem. Soc.* **2006**, *128* (22), 7390−7398.

(18) Bhavsar, G. A.; Asha, S. K. Pentadecyl Phenol- and Cardanol-Functionalized Fluorescent, Room-Temperature Liquid-Crystalline Perylene Bisimides: Effect of Pendant Chain Unsaturation on Self-Assembly. *Chem. - Eur. J.* **2011**, *17* (45), 12646−12658.

(19) Chen, Z. J.; Baumeister, U.; Tschierske, C.; Wurthner, F. Effect of core twisting on self-assembly and optical properties of perylene bisimide dyes in solution and columnar liquid crystalline phases. *Chem. - Eur. J.* **2007**, *13*, 450−465.

(20) Percec, V.; Peterca, M.; Tadjiev, T.; Zeng, X. B.; Ungar, G.; Leowanawat, P.; Aqad, E.; Imam, M. R.; Rosen, B. M.; Akbey, U.; Graf, R.; Sekharan, S.; Sebastiani, D.; Spiess, H. W.; Heiney, P. A.; Hudson, S. D. Self-Assembly of Dendronized Perylene Bisimides into Complex Helical Columns. *J. Am. Chem. Soc.* **2011**, *133* (31), 12197−12219.

(21) Zang, L.; Che, Y.; Moore, J. S. One-Dimensional Self-Assembly of Planar pi-Conjugated Molecules: Adaptable Building Blocks for Organic Nanodevices. *Acc. Chem. Res.* **2008**, *41* (12), 1596−1608.

(22) Weingarten, A. S.; Kazantsev, R. V.; Palmer, L. C.; Fairfield, D. J.; Koltonow, A. R.; Stupp, S. I. Supramolecular Packing Controls H-2 Photocatalysis in Chromophore Amphiphile Hydrogels. *J. Am. Chem. Soc.* **2015**, *137* (48), 15241−15246.

(23) Yang, Y.; Zhang, Y.; Wei, Z. Supramolecular Helices: Chirality Transfer from Conjugated Molecules to Structures. *Adv. Mater.* **2013**, *25* (42), 6039−6049.

(24) Echue, G.; Lloyd-Jones, G. C.; Faul, C. F. J. Chiral Perylene Diimides: Building Blocks for Ionic Self-Assembly. *Chem. - Eur. J.* **2015**, *21* (13), 5118−5128.

(25) Liu, M.; Zhang, L.; Wang, T. Supramolecular Chirality in Self-Assembled Systems. *Chem. Rev.* **2015**, *115* (15), 7304−7397.

(26) Huang, Y.; Hu, J.; Wei, Z.; Faul, C. F. J. Modulating helicity through amphiphilicity—tuning supramolecular interactions for the controlled assembly of perylenes. *Chem. Commun.* **2011**, *47*, 5554−5556.

(27) Hu, J.; Kuang, W.; Deng, K.; Zou, W.; Huang, Y.; Wei, Z.; Faul, C. F. J. Self-Assembled Sugar-Substituted Perylene Diimide Nanostructures with Homochirality and High Gas Sensitivity. *Adv. Funct. Mater.* **2012**, *22*, 4149−4198.

(28) Marty, R.; Nigon, R.; Leite, D.; Frauenrath, H. Two-Fold Odd-Even Effect in Self-Assembled Nanowires from Oligopeptide-Polymer-Substituted Perylene Bisimides. *J. Am. Chem. Soc.* **2014**, *136* (10), 3919−3927.

(29) Tidhar, Y.; Weissman, H.; Wolf, S. G.; Gulino, A.; Rybtchinski, B. Pathway-Dependent Self-Assembly of Perylene Diimide/Peptide Conjugates in Aqueous Medium. *Chem. - Eur. J.* **2011**, *17* (22), 6068−6075.

(30) Silly, F.; Shaw, A. Q.; Castell, M. R.; Briggs, G. A. D. A chiral pinwheel supramolecular network driven by the assembly of PTCDI and melamine. *Chem. Commun.* **2008**, No. 16, 1907−1909.

(31) Bai, S.; Debnath, S.; Javid, N.; Frederix, P. W. J. M.; Fleming, S.; Pappas, C.; Ulijn, R. V. Differential Self-Assembly and Tunable Emission of Aromatic Peptide Bola-Amphiphiles Containing Perylene Bisimide in Polar Solvents Including Water. *Langmuir* **2014**, *30* (25), 7576−7584.

(32) Xu, L.; Gao, D.; Song, J.; Shen, L.; Chen, W.; Chen, Y.; Zhang, S. Morphology-controlled self-assembly of an amphiphilic perylenetetracarboxylic diimide dimer-based semiconductor: from flower clusters to hollow spheres. *New J. Chem.* **2015**, *39* (7), 5553−5560.

(33) Wurthner, F.; Bauer, C.; Stepanenko, V.; Yagai, S. A black perylene bisimide super gelator with an unexpected J-type absorption band. *Adv. Mater.* **2008**, *20* (9), 1695−1698.

(34) Ghosh, S.; Li, X. Q.; Stepanenko, V.; Wurthner, F. Control of H- and J-Type pi Stacking by Peripheral Alkyl Chains and Self-Sorting Phenomena in Perylene Bisimide Homo- and Heteroaggregates. *Chem. - Eur. J.* **2008**, *14* (36), 11343−11357.

(35) Wang, K.-R.; An, H.-W.; Wang, Y.-Q.; Zhang, J.-C.; Li, X.-L. Multivalent glycoclusters constructed by chiral self-assembly of mannose functionalized perylene bisimide. *Org. Biomol. Chem.* **2013**, *11* (6), 1007−1012.

(36) Avinash, M. B.; Govindaraju, T. Amino Acid Derivatized Arylenediimides: A Versatile Modular Approach for Functional Molecular Materials. *Adv. Mater.* **2012**, *24* (29), 3905−3922.

(37) Cai, Y.; Guo, Z.; Chen, J.; Li, W.; Zhong, L.; Gao, Y.; Jiang, L.; Chi, L.; Tian, H.; Zhu, W.-H. Enabling Light Work in Helical Self-Assembly for Dynamic Amplification of Chirality with Photoreversibility. *J. Am. Chem. Soc.* **2016**, *138* (7), 2219−2224.

(38) Schmidt, C. D.; Boettcher, C.; Hirsch, A. Chiral Water-Soluble Perylenediimides. *Eur. J. Org. Chem.* **2009**, *31*, 5337−5349.

(39) Yagai, S.; Seki, T.; Karatsu, T.; Kitamura, A.; Wurthner, F. Transformation from H- to J-aggregated perylene bisimide dyes by complexation with cyanurates. *Angew. Chem., Int. Ed.* **2008**, *47* (18), 3367−3371.

(40) Seki, T.; Asano, A.; Seki, S.; Kikkawa, Y.; Murayama, H.; Karatsu, T.; Kitamura, A.; Yagai, S. Rational Construction of Perylene Bisimide Columnar Superstructures with a Biased Helical Sense. *Chem. - Eur. J.* **2011**, *17* (13), 3598−3608.

(41) Rieth, S.; Li, Z.; Hinkle, C. E.; Guzman, C. X.; Lee, J. J.; Nehme, S. I.; Braunschweig, A. B. Superstructures of Diketopyrrolopyrrole Donors and Perylenediimide Acceptors Formed by Hydrogen-Bonding and $\pi \cdots \pi$ Stacking. *J. Phys. Chem. C* **2013**, *117* (21), 11347−11356.

(42) Hoeben, F. J. M.; Zhang, J.; Lee, C. C.; Pouderoijen, M. J.; Wolffs, M.; Wurthner, F.; Schenning, A.; Meijer, E. W.; De Feyter, S. Visualization of Various Supramolecular Assemblies of Oligo(paraphenylenevinylene)-Melamine and Perylene Bisimide. *Chem. - Eur. J.* **2008**, *14* (28), 8579−8589.

(43) Thalacker, C.; Wurthner, F. Chiral perylene bisimide-melamine assemblies: Hydrogen bond-directed growth of helically stacked dyes with chiroptical properties. *Adv. Funct. Mater.* **2002**, *12* (3), 209−218.

(44) Syamakumari, A.; Schenning, A.; Meijer, E. W. Synthesis, optical properties, and aggregation behavior of a triad system based on perylene and oligo(p-phenylene vinylene) units. *Chem. - Eur. J.* **2002**, *8* (15), 3353−3361.

(45) Faul, C. F. J. Ionic Self-Assembly for Functional Hierarchical Nanostructured Materials. *Acc. Chem. Res.* **2014**, *47* (12), 3428−3438.

(46) Houbenov, N.; Nykänen, A.; Iatrou, H.; Hadjichristidis, N.; Ruokolainen, J.; Faul, C. F. J.; Ikkala, O. Fibrillar Constructs from Multilevel Hierarchical Self-Assembly of Discotic and Calamitic Supramolecular Motifs. *Adv. Funct. Mater.* **2008**, *18* (14), 2041−2047.

(47) Guan, Y.; Yu, S. H.; Antonietti, M.; Bottcher, C.; Faul, C. F. J. Synthesis of supramolecular polymers by ionic self-assembly of oppositely charged dyes. *Chem. - Eur. J.* **2005**, *11* (4), 1305−1311.

(48) Everett, T. A.; Twite, A. A.; Xie, A. F.; Battina, S. K.; Hua, D. H.; Higgins, D. A. Preparation and characterization of nanofibrous perylene-diimide - Polyelectrolyte composite thin films. *Chem. Mater.* **2006**, *18* (25), 5937−5943.

(49) Faul, C. F. J.; Antonietti, M. Ionic self-assembly: Facile synthesis of supramolecular materials. *Adv. Mater.* **2003**, *15* (9), 673−683.

(50) Franke, D.; Vos, M.; Antonietti, M.; Sommerdijk, N.; Faul, C. F. J. Induced supramolecular chirality in nanostructured materials: Ionic self-assembly of perylene-chiral surfactant complexes. *Chem. Mater.* **2006**, *18* (7), 1839−1847.

(51) Huang, Y. W.; Yan, Y.; Smarsly, B. M.; Wei, Z. X.; Faul, C. F. J. Helical supramolecular aggregates, mesoscopic organisation and nanofibers of a perylenebisimide-chiral surfactant complex via ionic self-assembly. *J. Mater. Chem.* **2009**, *19* (16), 2356−2362.

(52) Jancy, B.; Asha, S. K. Hydrogen-bonding-induced conformational change from J to H aggregate in novel highly fluorescent liquid-crystalline perylenebisimides. *Chem. Mater.* **2008**, *20* (1), 169−181.

(53) Wang, W.; Wan, W.; Zhou, H. H.; Niu, S. Q.; Li, A. D. Q. Alternating DNA and pi-conjugated sequences. Thermophilic foldable polymers. *J. Am. Chem. Soc.* **2003**, *125* (18), 5248−5249.

(54) Wang, W.; Han, J. J.; Wang, L. Q.; Li, L. S.; Shaw, W. J.; Li, A. D. Q. Dynamic pi-pi stacked molecular assemblies emit from green to red colors. *Nano Lett.* **2003**, *3* (4), 455−458.

(55) Xue, L.; Wang, Y. F.; Chen, Y. L.; Li, X. Y. Aggregation of wedge-shaped perylenetetracarboxylic diimides with a different number of hydrophobic long alkyl chains. *J. Colloid Interface Sci.* **2010**, *350* (2), 523−529.

(56) Chen, Z. J.; Stepanenko, V.; Dehm, V.; Prins, P.; Siebbeles, L. D. A.; Seibt, J.; Marquetand, P.; Engel, V.; Wurthner, F. Photoluminescence and conductivity of self-assembled pi-pi stacks of perylene bisimide dyes. *Chem. - Eur. J.* **2007**, *13* (2), 436−449.

(57) Kasha, M.; Rawls, H. R.; El-Bayoumi, M. A. The exciton model in molecular spectroscopy. *Pure Appl. Chem.* **1965**, *11*, 371−392.

(58) Fennel, F.; Wolter, S.; Xie, Z.; Ploetz, P.-A.; Kuehn, O.; Wuerthner, F.; Lochbrunner, S. Biphasic Self-Assembly Pathways and Size-Dependent Photophysical Properties of Perylene Bisimide Dye Aggregates. *J. Am. Chem. Soc.* **2013**, *135* (50), 18722−18725.

(59) Wu, H. X.; Xue, L.; Shi, Y.; Chen, Y. L.; Li, X. Y. Organogels Based on J- and H-Type Aggregates of Amphiphilic Perylenetetracarboxylic Diimides. *Langmuir* **2011**, *27* (6), 3074−3082.

(60) Kumar, J.; Nakashima, T.; Tsumatori, H.; Kawai, T. Circularly Polarized Luminescence in Chiral Aggregates: Dependence of Morphology on Luminescence Dissymmetry. *J. Phys. Chem. Lett.* **2014**, *5* (2), 316−321.